New Journal of Physics
The open access journal at the forefront of physics

Deutsche Physikalische Gesellschaft DPG IOP Institute of Physics

PAPER • OPEN ACCESS

Molecular interferometers: effects of Pauli principle on entangled-enhanced precision measurements

To cite this article: P Alexander Bouvrie *et al* 2019 *New J. Phys.* **21** 123011

New Journal of Physics
The open access journal at the forefront of physics

Deutsche Physikalische Gesellschaft DPG
IOP Institute of Physics

Published in partnership with: Deutsche Physikalische Gesellschaft and the Institute of Physics

CrossMark

OPEN ACCESS

RECEIVED
15 August 2019

REVISED
6 November 2019

ACCEPTED FOR PUBLICATION
25 November 2019

PUBLISHED
12 December 2019

PAPER

Molecular interferometers: effects of Pauli principle on entangled-enhanced precision measurements

P Alexander Bouvrie[1,5], Ana P Majtey[2,3], Francisco Figueiredo[1] and Itzhak Roditi[1,4]

[1] Centro Brasileiro de Pesquisas Físicas, Rua Dr. Xavier Sigaud 150, 22290-180 Rio de Janeiro, Brazil
[2] Facultad de Matemática, Astronomía y Física, Universidad Nacional de Córdoba, Av. Medina Allende s/n, Ciudad Universitaria, X5000HUA Córdoba, Argentina
[3] Consejo de Investigaciones Científicas y Técnicas de la República Argentina, Av. Rivadavia 1917, C1033AAJ, Ciudad Autónoma de Buenos Aires, Argentina
[4] Institute for Theoretical Physics, ETH Zurich 8093, Switzerland
[5] Author to whom any correspondence should be addressed.

E-mail: bouvrie@ugr.es

Keywords: molecular BEC, fermion interference, quantum metrology

Abstract

Feshbach molecules forming a Bose–Einstein condensate (BEC) behave as non-ideal bosonic particles due to their underlying fermionic structure. We study the observable consequences of the fermion exchange interactions in the interference of molecular BECs for entangled-enhanced precision measurements. Our many-body treatment of the molecular condensate is based on an ansatz of composite two-fermion bosons which accounts for all possible fermion exchange correlations present in the system. The Pauli principle acts prohibitively on the particle fluctuations during the interference process leading to a loss of precision in phase estimations. However, we find that, in the regime where molecular dissociations do not jeopardize the interference dynamics, measurements of the phase can still be performed with a precision beyond the classical limit comparable to atomic interferometers. We also show that the effects of Pauli principle increases with the noise of the particle detectors such that molecular interferometers would require more efficient detectors.

1. Introduction

Modern interferometers exploiting particle entanglement are among the most precise measurement devices used so far. They provide a remarkable tool for high precision metrology that have been successfully used, e.g. to detect gravitational waves [1, 2]. Small changes of the quantity to be measured due to the external conditions are mapped to changes of the relative phase of the interference between two photonic or atomic modes. The sensitivity with respect to these changes increases with N, the total number of particle involved in the interference.

For interferometers with uncorrelated particles sources, the minimum phase uncertainty is limited by the shot noise, a trace of the particle nature of quantum waves. However, the shot noise limit (also called standard quantum limit), for which the maximal phase precision scales as $\Delta\theta_{\mathrm{sn}} \propto 1/\sqrt{N}$, can be overcome by using entangled particle resources, such as spin squeezed states [3]. The ultimate Heisenberg limit, where the phase uncertainty scales linearly with the number of particles $\Delta\theta_{\mathrm{H}} \propto 1/N$, can be achieved in the limit of infinite squeezing, where the squeezed states become identical to twin Fock states [4].

Twin Fock states, i.e. states with two orthogonal modes populated by the same number of particles, have been produced with both, photons [4, 5] and ultracold bosonic atoms [6–8]. However, entangled-enhanced precision measurements of the resulting interference phase have been performed only in the case of ultracold bosonic atoms [6, 8]. This is mainly because current twin photon beams experiments have much higher particle losses than experiments with twin matter waves.

Another interesting source of coherent wave matter, not exploited yet for quantum metrology, are utracold interacting Fermi gases in the molecular Bose–Einstein condensate (mBEC) regime [9, 10], since its lifetime in experiments is much longer than atomic BECs [11, 12]. Interacting bosonic and fermionic atoms behaves extremely different at low temperatures [13], because the Pauli exclusion principle between identical fermions does not allow multiple occupations of the single-particle states of the system. However, in unpolarized two-component ultracold Fermi gases, the Pauli exclusion principle can be circumvented by tunning the interaction between different fermion species. Increasing the (attractive) interaction, fermions bind together forming diatomic molecules, which in the limit of maximum interaction/binding become perfect bosonic molecules [14]. In this strong binding limit all fermion-pairs condense to the same molecular ground state forming a perfect mBEC, whereas weakly bonded molecules leads to quantum depletion of the condensate [15, 16].

The mBECs are composed by N identical pairs of distinguishable fermionic atoms A and B. The quantum depletion of the condensate is a consequence of the fermion exchange interactions between identical (indistinguishable) fermionic atoms A or B [17]. It can be easily confused in the experiments with particle loss effects when only the condensate component is measured without taking into account the total number of particles of the system [18]. Moreover, it is not known how these exchange interactions between identical fermions affect the system's ability to perform metrology beyond the standard quantum limit.

Here, we show the effects of quantum depletion on the phase estimation of two interfering mBECs, essential for future high precision experiments using mBECs. We consider initially prepared twin Fock states in two orthogonal molecular modes, and a interferometric dynamics which is determined by a single parameter, namely, the interference phase θ. The initial twin Fock state of mBECs is obtained by using an ansatz of composite bosons [19] applied to the ^{6}Li Feshbach resonance [17].

We found that condensate depletion reduces the odd/even discrete structure of the typical U-shaped particle distribution that arise when measuring the different numbers of particles populating both modes. Such an odd/even fluctuation reduction is very similar to that caused by particle losses [5, 6, 8]. Condensate depletion also renders the standard deviation of the interfering mBECs to be smaller, as compared with the one given by the ideal BECs interference of bosonic atoms. The phase uncertainty increases with respect to the ideal bosonic case, with the consequent loss of precision in phase estimations. However, we show that the increase in phase uncertainty is not so significant such that entanglement-enhanced precision measurements are also feasible with mBECs. This is because the U-shape of the particle distribution, indicating many-particle entanglement [5, 6], is preserved for small values of the interference phase $\theta \ll 1$. We also analyze the phase uncertainty considering a Gaussian noise in the particle detectors, and show how the effects of quantum depletion increase with the detection noise. Therefore, molecular interferometers would require more efficient detectors to reach sub-shot noise precision measurements.

The article is organized as follows. We introduce the coboson ansatz and its application to two-component Fermi gases in section 2. We thoroughly discuss in section 3 the interference dynamics that we consider for ultracold interacting Fermi gases trapped in a double well potential. In section 4 we show the population imbalance and the standard deviation of two interfering mBECs for different values of the interaction parameter and analyze the effects of the condensate depletion. In section 5 we calculate the phase estimation uncertainty which is inferred from the sensitivity of the state to small rotations around $\hat{J}_z$ axis given by a spin representation $\hat{\mathbf{J}} = (\hat{J}_x, \hat{J}_y, \hat{J}_z)$ compatible with interference dynamics. Finally, in section 6 we provide a discussion of the results and summarize our conclusions.

2. Coboson ansatz for interacting Fermi gases

Feshbach resonance provides a way to tune the scattering length a characterizing interaction between different fermion species, A and B, of a two-component ultracold Fermi gas [13]. This allowed the experimental realization of the BEC–BCS (Bardeen–Cooper–Schrieffer) crossover with ultracold atomic gases [20]. In the molecular BEC regime, the ground state at zero temperature can be described by pair correlated states, also called coboson (composite bosons) states [17, 21, 22]. The cobosons ansatz is given by the successive application of a complex creation operator $\hat{c}^\dagger$ on the vacuum

$$|N\rangle = \frac{(\hat{c}^\dagger)^N}{\sqrt{N!\chi_N}}|0\rangle, \tag{1}$$

where χ_N is the normalization factor [23]. The operator $\hat{c}^\dagger$ creates a two-fermion composite particle as a function of the elementary fermionic creation operators $\hat{a}_j^\dagger$ and $\hat{b}_j^\dagger$, $\hat{c}^\dagger = f(\hat{a}_1^\dagger, \hat{b}_1^\dagger, \hat{a}_2^\dagger, \hat{b}_2^\dagger, \ldots)$.

Particularly, we use a novel approach to find the function f starting from scratch in the ladder of Fock states [17]. It considers that the operator $\hat{c}^\dagger$ acting on the vacuum creates a pair of fermions in the ground state of an harmonically trapped Feshbach molecule, $\hat{c}^\dagger|0\rangle = |\psi_{\text{g.s.}}\rangle$. This approach uses jointly first and second quantization formalisms of quantum mechanics in an original way. The ground state $|\psi_{\text{g.s.}}\rangle$ of a ^{6}Li molecule is computed analytically using a two-state model in continuous variables (first quantization) [13]. Then, we calculate the Schmidt decomposition of the state, i.e.

$$|\psi_{\rm g.s.}\rangle = \sum_{j=1}^{S}\sqrt{\lambda_j}\,|a_j\rangle\,|b_j\rangle, \tag{2}$$

where $|a_j\rangle$ and $|b_j\rangle$ are the single-fermion states of the system associated to each fermion species. The two different species can be identified as two different hyperfine or spin states of the constituent fermionic atoms of a molecule. Considerations of the indistinguishability between the two fermion are also included in this formalism, since the spin component of the two fermion state would be the antisymmetric singlet $|a_j\rangle\,|b_j\rangle = \phi_j(\vec{r}_a)\phi_j(\vec{r}_b)(|\uparrow\rangle_a|\downarrow\rangle_b - |\downarrow\rangle_a|\uparrow\rangle_b)/\sqrt{2}$. The Schmidt coefficient distribution $\Lambda = (\lambda_1, \lambda_2, \ldots, \lambda_S)$ is computed numerically and depends on the ratio between the size of the trap L and the scattering length a, $\Lambda = \Lambda(L/a)$. It fulfills $\sum_{j=1}^{S}\lambda_j \approx 1$, being $S \approx 10^6$ the Schmidt rank.

With the state (2) at hand, the cobosons creation operator (second quantization formalism) is naturally defined as $\hat{c}^\dagger \equiv \sum_{j=1}^{S}\sqrt{\lambda_j}\,\hat{a}_j^\dagger\,\hat{b}_j^\dagger$ [24]. The elementary fermion operators $\hat{a}_j^\dagger$ ($\hat{b}_j^\dagger$) creates a fermion A (B) in the single-fermion state $|a_j\rangle$ ($|b_j\rangle$). Since $(\hat{a}_j^\dagger)^2 = (\hat{b}_j^\dagger)^2 = 0$ because of Pauli principle,

$$|N\rangle = \frac{1}{\sqrt{N!\chi_N}}\sum_{\substack{j_1, j_2, \cdots, j_N = 1\\ \sigma(j_1, \ldots, j_N)}}^{S}\left(\prod_{k=1}^{N}\sqrt{\lambda_{j_k}}\,\hat{a}_{j_k}^\dagger\,\hat{b}_{j_k}^\dagger\right)|0\rangle, \tag{3}$$

where $\sigma(j_1, \ldots, j_N)$ indicates that the indices $j_1, j_2, \ldots, j_N$ must take distinct values in the sum over all the indices appearing in above equation (3), and $|0\rangle \equiv \bigotimes_{j=1}^{S}|\text{vac}\rangle_{a_j} \otimes |\text{vac}\rangle_{b_j}$ is the vacuum. Note that the restriction $\sigma(j_1, \ldots, j_N)$ guarantees the Pauli exclusion principle, i.e. there are not two labels with the same value. Using the Schmidt base given by equation (2), the N-coboson normalization factor χ_N is given by the elementary symmetric polynomial [25]

$$\chi_N = N!\sum_{1 \leqslant j_1 < j_2 < \cdots < j_N \leqslant S}\lambda_{j_1}\lambda_{j_2}\cdots\lambda_{j_N}. \tag{4}$$

Ensembles with large number of ultracold interacting fermions exhibit an universal behavior with the interaction parameter $k_F a$. The Fermi wave number of a non-interacting gas is $k_F = (6\pi^2 n)^{1/3}$, with $n = N/V$ being the atom-pair density and $V = 4\pi L^3/3$ the volume of the system. Thus, the ensemble of fermionic atoms (in the ground state $|N\rangle$) and observables, are controlled by the parameter $k_F a$, which is the ratio between the characteristic length of the interaction and the density of states.

In this work, we assume an initially prepared entangled twin Fock state of mBECs

$$|\Psi\rangle = |M\rangle_1|M\rangle_2 = \frac{(\hat{c}_1^\dagger)^M}{\sqrt{M!\chi_M}}\frac{(\hat{c}_2^\dagger)^M}{\sqrt{M!\chi_M}}|0\rangle_1|0\rangle_2. \tag{5}$$

This state has two molecular modes, 1 and 2, equally populated by $M = N/2$ fermion pairs. The preparation of Twin Fock states with molecular wave matter has not been experimentally achieved yet. Progress towards the manipulation of ultracold interacting Fermi gases opened the possibility to produce coherently, or independently, two BECs [18]. But the resulting states are yet characterized by uncorrelated particle fluctuations between the modes. Nevertheless, equation (5) is the ground state of a Hamiltonian describing two ultracold interacting Fermi gases in two independent modes with zero tunneling rate between modes, and one would expect that twin Fock states could be generated by some kind of quantum phase transition, as performed with bosonic atoms [7].

3. Interference dynamics

The dynamics of two interfering ultracold interacting Fermi gases can be very complicated in general. However, in the strong-binding regime, ultracold fermionic atoms co-tunnel between two separated traps as pairs [26–28]. Moreover, the coherent splitting of an unpolarized mBEC (with the same number of atoms of each species) in the regime $1/(k_F a) \geqslant 1$ yields two unpolarized mBECs [18], showing that a bi-fermion approximation also holds for large ensembles of ultracold fermionic atoms. Fermion-pairs in the BEC regime can be represented, therefore, by using single-bi-fermion creation operator $\hat{d}_{q,j}^\dagger = \hat{a}_{q,j}^\dagger\hat{b}_{q,j}^\dagger$ with $q = 1, 2$ [29–31].

Let consider twin mBECs prepared in two identical traps where a fermion-pair in the state i of mode q is allowed to co-tunnel to the state j of mode $3 - q$ with tunneling rate α_{ij}. Assuming that α_{ij} is larger than any other pair energy of the system except the molecular binding energy $U_{\rm mol}$, the dynamics of the system would be approximately generated by the Hamiltonian

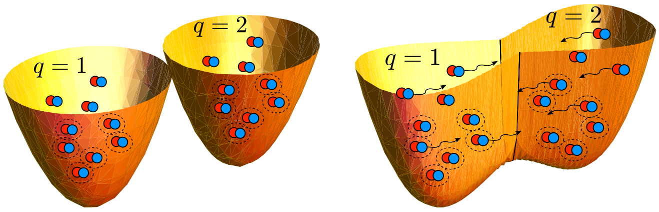

Figure 1. (Left) Representation of an interacting Fermi gas in the molecular BEC regime prepared in a double well potential. Fermion pairs are allowed to co-tunnel between the traps by deforming the trapping potential (right). A global phase dynamics might be achieved by shaping properly the tunnel which couples the wells (black solid line). Oval dashed lines represent the Pauli principle between fermions of the molecules and the zigzagged arrows indicate fermion pairs that are allowed to co-tunnel.

$$\hat{H} = \sum_{i,j=1}^{S} \frac{\alpha_{ij}^2}{2U_{\mathrm{mol}}} (\hat{d}_{1,i}^{\dagger}\hat{d}_{2,j} + \hat{d}_{2,i}^{\dagger}\hat{d}_{1,j}). \tag{6}$$

Because of the high degeneracy of the fermionic gas, many off-diagonal terms in the above sums are non-zero, i.e. $\alpha_{ij} \neq 0$ for degenerated states i and j (states with equal single-fermion energies $E_i^{(A/B)} = E_j^{(A/B)}$). While for non-degenerated states i and j $\alpha_{ij} = 0$, because of energy conservation during the dynamic. The off-diagonal terms contribute to avoid the Pauli principle, since the larger the degeneracy of the state i the larger the number of states j to which pairs can tunnel fulfilling energy conservation. Therefore, these off-diagonal terms would contribute to increase the phase resolution. In this work, we consider $\alpha_{ij} = 0\ \forall\, i \neq j$, then our results actually constitute a lower bound of the phase resolution. An alternative to make the effects of the quantum depletion more visible would be to consider an anisotropic trap as it presents a lower degree of degeneracy.

The diagonal terms, α_{jj}, i.e. the coupling between the jth states of both modes can have, in general, different values depending on the shape of the trapping potentials and the 'tunnel' coupling both traps, see figure 1. The existence of a global phase in the dynamics depends, in fact, on these diagonal terms ($i = j$) in the sums of equation (6). From the infinite possible configurations producing a global phase dynamics we consider the simplest one, $\alpha_{jj} = J_0\ \forall\ j$. That is, we approximate the Hamiltonian (6) by

$$\hat{H} \approx \frac{J}{2} \sum_{j=1}^{S} (\hat{d}_{1,j}^{\dagger}\hat{d}_{2,j} + \hat{d}_{2,j}^{\dagger}\hat{d}_{1,j}), \tag{7}$$

where $J = \alpha_{ii}^2/U_{\mathrm{mol}}$ is the rescaled tunneling rate. A global phase dependence arise in the state evolution

$$\mathrm{e}^{-\mathrm{i}t\hat{H}}|M\rangle_1|M\rangle_2 \approx \prod_{j=1}^{S} \mathrm{e}^{-\mathrm{i}\theta/2(\hat{d}_{1,j}^{\dagger}\hat{d}_{2,j} + \hat{d}_{2,j}^{\dagger}\hat{d}_{1,j})}|M\rangle_1|M\rangle_2, \tag{8}$$

where the interference phase is given by $\theta = tJ$, being t the time evolution.

Even though fermions co-tunnel as pairs in the BEC regime through the simple dynamics induced by the Hamiltonian (7), it is not clear that there is a well defined operator dynamic describing the interference processes (8). This is because couplings between modes 1 and 2 are neglected by Pauli principle when two fermion-pairs occupy the same internal state j of the modes. The problem was solved by using a superposition representation of the composite boson state in terms of states with a different number of elementary bosons and fermions [32]: Exploiting its symmetry, the initial state (5) can be written as

$$|M\rangle_1|M\rangle_2 \simeq \sum_{p=0}^{M} \sqrt{\omega_p}\,|\phi_p(0)\rangle, \tag{9}$$

where the states $|\phi_p(0)\rangle$ are orthogonal. The state $|\phi_p(0)\rangle$ represents $2p$ fermion-pairs that behave as elementary fermions, holding always coincident events in interferometric modes $q = 1$ and $q = 2$, and $N - 2p$ fermion-pairs that are distributed as elementary bosons. Their corresponding weights are given by

$$w_p = \binom{M}{p}^2 \frac{p!}{\chi_M^2}\, \Omega(\{\underbrace{2,\ldots,2}_{p}, \underbrace{1,\ldots,1}_{N-2p}\}). \tag{10}$$

where Ω is a symmetric polynomial in $\boldsymbol{\Lambda}$. The polynomial Ω can be computed for relative large $N \lesssim 50$ using the power sums $\mathcal{M}(m) = \sum_j \lambda_j^m$ and the recurrence formula [32]

$$\Omega(\{x_1 \ldots x_N\}) = \mathcal{M}(x_1)\Omega(\{\underbrace{x_2 \ldots x_N}_{N-1}\}) - \sum_{m=2}^{N} \Omega(\{\underbrace{x_1 + x_m, x_2, \ldots, x_{m-1}, x_{m+1}, \ldots, x_N}_{N-1}\}). \tag{11}$$

The twin Fock state evolves as

$$e^{-it\hat{H}}|M\rangle_1|M\rangle_2 \simeq \sum_{p=0}^{M} \sqrt{\omega_p}|\phi_p(t)\rangle, \tag{12}$$

and the probability to find m fermion pairs in the mode 1 (and $N - m$ in mode 2) at time t is given by

$$\mathcal{P}(m) = \sum_{p=0}^{\mathrm{Min}\{m,N-m\}} \omega_p \mathcal{P}(m, p), \tag{13}$$

with $\mathcal{P}(m, p) = |\langle\phi_p(0)|\phi_p(t)\rangle|^2$ being the probability to find m fermion pairs in one of modes, where p of them behaves as fermions and $m - p$ as bosons. The probability

$$\mathcal{P}(m, p) = |\mathcal{A}(n_1, n_2, m_1, m_2)|^2, \tag{14}$$

where $n_1 = n_2 = M - p$ are the effective number of bosons in the inputs and $m_1 = m - p$ and $m_2 = N - m - p$ the effective number of bosons in the outputs, respectively, can be evaluated with the methods presented in [33–35]. The amplitudes $\mathcal{A}$ of two interfering Fock states of elementary bosons was computed as

$$\mathcal{A}(n_1, n_2, m_1, m_2) = \sqrt{n_1!n_2!m_1!m_2!}\,\frac{(\sqrt{T})^{m_2+n_1}}{(\mathrm{i}\sqrt{R})^{n_1-m_1}} \times \sum_{q=\mathrm{Max}[0,n_1-m_1]}^{\mathrm{Min}[n_1,m_2]} \frac{(-1)^q(R/T)^q}{(n_1-q)!(m_1-n_1+q)!q!(m_2-q)!}. \tag{15}$$

The reflection and transmission coefficients are $R = \cos^2(\theta/2)$ and $T = \sin^2(\theta/2)$, respectively.

Since elementary fermions are always equally distributed in both modes, only fermion pairs that behave as bosons contribute to the particle fluctuations. This is reflected in equation (14) by the dependence on θ solely of the ideal $(N - 2p)$-boson contribution. Reminiscences of the underlying fermionic structure of the molecules are thus reflected in the interference of mBECs as a partially fermionic behavior of the collective wave function. Since partially fermionic behavior translates into particle fluctuation suppressions, we expect less precision in the interference phase estimation by using molecular BECs than atomic BECs.

4. Populations imbalance

By introducing the global fermion spin operator $\hat{\mathbf{J}} = (\hat{J}_x, \hat{J}_y, \hat{J}_z)$ [36] the Hamiltonian (7) can be written in terms of the $\hat{J}_x$ spin component

$$\hat{J}_x = \frac{1}{2}\sum_{j=1}^{S}(\hat{d}_{1,j}^{\dagger}\hat{d}_{2,j} + \hat{d}_{2,j}^{\dagger}\hat{d}_{1,j}), \tag{16}$$

such that $\hat{H} \approx J\hat{J}_x$. The population imbalance of the system is given by the $\hat{J}_z$ spin-like component operator

$$\hat{J}_z = \frac{1}{2}\sum_{j=1}^{S}(\hat{d}_{1,j}^{\dagger}\hat{d}_{1,j} - \hat{d}_{2,j}^{\dagger}\hat{d}_{2,j}), \tag{17}$$

which is the fermionic analogous of the usual spin $\hat{J}_z$ component given by the Schwinger representation. Fluctuations of the difference of the particle number, namely, $\langle\hat{J}_z^2\rangle$ and $\langle(\Delta\hat{J}_z^2)^2\rangle = \langle\hat{J}_z^4\rangle - \langle\hat{J}_z^2\rangle^2$, are the experimental observables required for the estimation of the phase and its uncertainty, respectively. The above defined operators $\hat{J}_x$ and $\hat{J}_z$ together with

$$\hat{J}_y = \frac{1}{2i}\sum_{j=1}^{S}(\hat{d}_{1,j}^{\dagger}\hat{d}_{2,j} - \hat{d}_{2,j}^{\dagger}\hat{d}_{1,j}), \tag{18}$$

fulfill the commutation relation $[\hat{J}_i, \hat{J}_j] = \mathrm{i}\varepsilon_{ijk}\hat{J}_k$ for the Lie SU(2) algebra.

In figure 2(a), we show the typical standard deviation

$$\sigma(\hat{J}_z/N) = \frac{\sqrt{\langle\hat{J}_z^{\,2}\rangle - \langle\hat{J}_z\rangle^2}}{N} \tag{19}$$

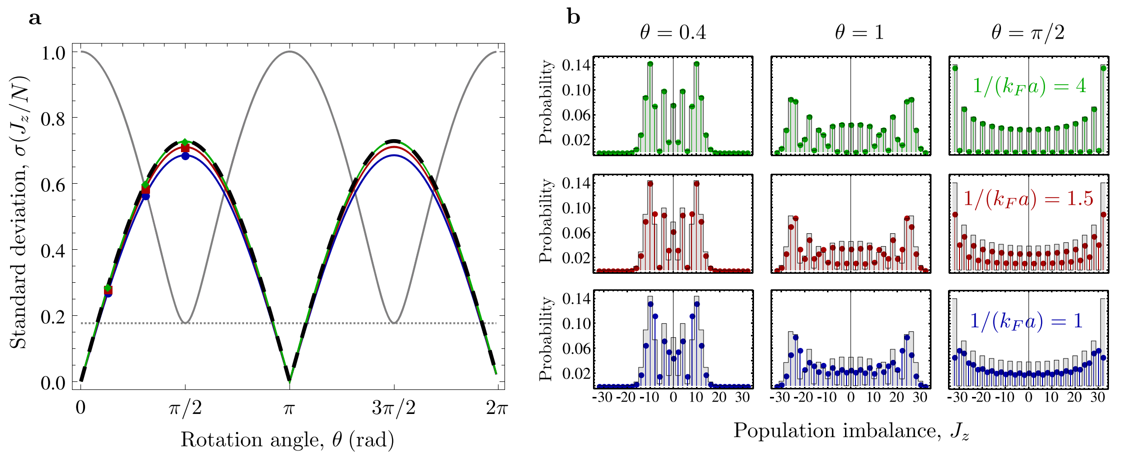

Figure 2. (a) Fluctuations of the normalized population imbalance for an initial twin Fock state of $N = 32$ fermion pairs with characteristic interaction parameter $1/(k_F a) = 1.0,\ 1.5$ and 4.0 (blue, red and green solid lines, respectively). Black dashed line corresponds to the standard deviation $\sigma(\hat{J}_z/N)$ of an ideal bosonic interference of entangled twin Fock states, while gray lines corresponds to the standard deviation for two initial source of unentangled atoms, namely, the single atomic Fock state (solid) and the coherent state (the quantum states generated by coherent splitting of a quantum mode) (dotted). The standard deviation of a molecular twin Fock state oscillates as $\mathcal{V}|\sin(\theta)|$ where $\mathcal{V}$ increases with $1/(k_F a)$. (b) Distribution of the population imbalance $\hat{J}_z$ (probability distributions of the state over the $\hat{J}_y$ Dicke eigenbases) for three different values of the phase interference $\theta = 0.4$, 1 and $\pi/2$ and of the interaction parameter $1/(k_F a)$. These values correspond with the dots depicted in figure (a). The gray shaded histogram is the ideal bosonic distribution of the population imbalance.

of the normalized population imbalance $\hat{J}_z/N$ of two unentangled state, namely, the single-mode Fock state $|N\rangle_1|0\rangle_2$ (gray solid), and the state resulting from the coherent splitting of a Fock state $|N\rangle$ [30, 31] (gray dotted). For both unentangled states the resulting standard deviation is the same as for unentangled states of elementary bosons. For initially prepared entangled twin Fock states, the relative particle number uncertainty vanishes ($\sigma(\hat{J}_z/J) = 0$) such that the relative phase is completely undetermined. A reduction of the phase uncertainty on the output measurements beyond shot-noise limit is attained at the expense of increasing the uncertainty of the observables. The extreme case is therefore attained with twin Fock states for which the standard deviation vanishes at $\theta = 0,\ \pi,\ 2\pi,\ldots$ (black dashed line for elementary bosons and solid lines with colors for molecular BECs with different interaction parameter $k_F a$).

Depletion in the BEC regime, is a consequence of fermion exchange interactions among the constituent of the identical molecules, and it is reflected as a partially fermionic behavior in the interference. In figure 2(a) we show the standard deviation of two interfering mBECs with $N = 32$ fermion pairs and interaction parameter $1/(k_F a) = 1,\ 1.5$ and 4 (red, blue and green solid lines, respectively). For increasing values of the interaction parameter $k_F a$, the depletion of the condensates increases, and the standard deviation decreases as a consequence of fermionic fluctuation suppressions. Particularly, the partially fermionic behavior induces suppression of even/odd fluctuations, see figure 2(b). For $1/(k_F a) = 4$ (Green dots) the probability of the different population imbalances match the ideal bosonic behavior (gray shaded histogram), whereas for $1/(k_F a) = 1$ the even/odd particle fluctuations almost vanishes. Particle losses and/or the absence of single-particle resolution in the experiments also render even/odd fluctuations vanishes [5, 6]. Nevertheless, the U-shape of the probability distribution, considered in the literature as an indicator for possible entanglement-enhanced phase resolution [4–8], is preserved.

5. Phase uncertainty

Interferometers with uncorrelated atoms are fundamentally limited by shot noise. The best possible precision for uncorrelated resources is given by the classical Cramer–Rao bound of parameter estimation, the maximal interferometric phase precision for ν independent measurements is given by $\Delta\theta_{\rm SN} = 1/\sqrt{\nu N}$. This limit can be surpass by creating entanglement between the atoms. Twin Fock states are maximally correlated states in particle numbers. The redistribution of particle in both modes during the interference is strongly affected by the entanglement, allowing sub-shot-noise sensitivities in measurements of the relative phase θ. The ultimate limit to the phase precision, the so-called Heisenberg limit, where the sensitivity scales as $\Delta\theta_{\rm H} = 1/(\sqrt{\nu}N)$, can be achieved using twin Fock states.

A typical interference process is given by a rotation of the input state by an angle θ, which represent the relative phase of the condensates. This rotation angle can be mapped onto the population imbalance by using the complete set of observables (16)–(18), which can be experimentally measured. Since for twin Fock states the

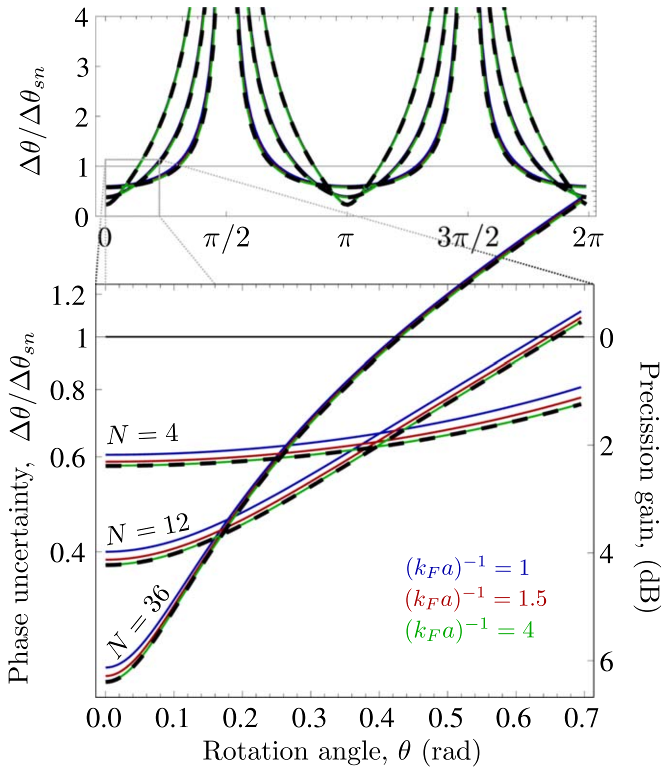

Figure 3. Phase uncertainty $\Delta\theta$ with respect to shot noise $\Delta\theta_{sn}$ of a twin Fock interferometry realized with molecular Bose–Einstein condensates, as a function of the interference phase θ and for $N = 4, 12$ and 36. The lower figure is an amplification of the upper one within the phase range [0, 0.7]. The phase uncertainty beats the standard quantum limits $\Delta\theta/\Delta\theta_{sn} = 1$, and decreases with the interaction parameter $(k_F a)^{-1} = 1.0,\ 1.5$ and 4.0 (blue, red and green solid lines, respectively). Deviation from the ideal bosonic behavior (black dashed lines) are caused by a reduction of even–odd particle fluctuations (see figure 2(b)) caused by the Pauli blocking between fermion pairs.

relative phase θ is completely undetermined, a rotation of these states maps the quantity of interest on the expectation value of the output fluctuations $\langle \hat{J}_z^2 \rangle$ instead of $\langle \hat{J}_z \rangle$ [37]. The phase estimation uncertainty is evaluated from the error propagation equation as [38]

$$\Delta\theta = \frac{\sqrt{\langle \hat{J}_z^4 \rangle - \langle \hat{J}_z^2 \rangle^2}}{\sqrt{\nu} \left| \frac{\mathrm{d}\langle \hat{J}_z^2 \rangle}{\mathrm{d}\theta} \right|}, \tag{20}$$

where the mean value of the of the operator $\hat{J}_z^\alpha$ is given by

$$\langle \hat{J}_z^\alpha \rangle = \sum_{m=0}^{N} (N - 2m)^\alpha \mathcal{P}(m). \tag{21}$$

The phase uncertainty (20) for a twin Fock state beats the standard quantum limit $\Delta\theta_{sn}$ for values of the relative phase close to $\theta = 0, \pi, 2\pi, \ldots$, see figure 3(a). In the expanded figure 3(b), we also show the phase uncertainty with respect to the shot-noise limit $\Delta\theta/\Delta\theta_{sn}$ as a function of θ, and it can be appreciated the deviation of this magnitude caused by partially fermionic behavior. From this figure we infer that high metrological precision is reached, beating the standard quantum limit for all values of $1/(k_F a) > 1$. Slightly increasing θ, the deviation from the ideal bosonic behavior decreases if the number of particle is large enough, for instance $N = 36$, see figure 3(b). This is an important remark, since noise in the experimental particle detection allows one to reach sub-shot noise resolutions only for relatively small $\theta > 0$ [6, 8].

Particle detectors are subject to an intrinsic noise. For atomic BEC interferometers, such a noise is much larger than any other source of precision loss, e.g. sources of error due to statistical mixtures of the prepared twin Fock state [6, 8]. Assuming a Gaussian detection noise σ_{dn} when measuring the population imbalance $\hat{J}_z$ we have

$$\langle \hat{J}_z^2 \rangle_{gdn} = \langle \hat{J}_z^2 \rangle + \sigma_{dn}^2 \tag{22}$$

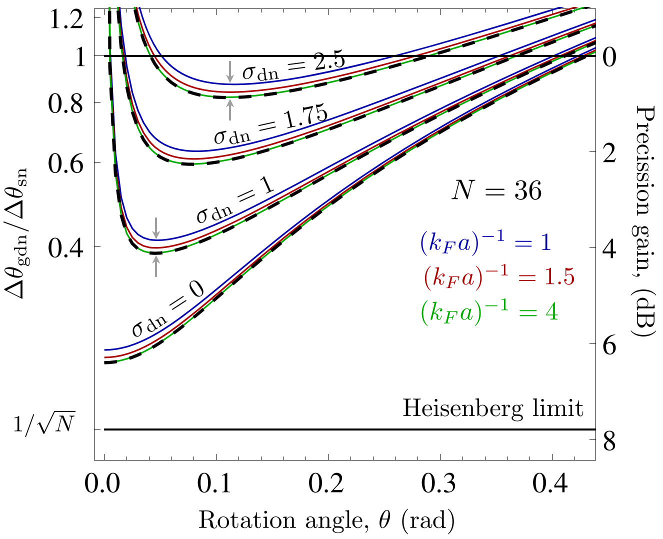

Figure 4. Phase uncertainty $\Delta\theta_{\mathrm{gdn}}$ with respect to shot noise $\Delta\theta_{\mathrm{sn}}$ of a twin Fock interferometry of molecular Bose–Einstein condensates with $N = 36$ and a Gaussian detection noise of $\sigma_{\mathrm{dn}} = 0, 1, 2$, and 3 fermion pairs. Horizontal lines are the standard quantum limit, $\Delta\theta/\Delta\theta_{\mathrm{sn}} = 1$, and the Heisenberg limit, $1/\sqrt{N}$.

and

$$\langle \hat{J}_z^4 \rangle_{\mathrm{gdn}} = \langle \hat{J}_z^4 \rangle + 6\sigma_{\mathrm{dn}}^2 \langle \hat{J}_z^2 \rangle + \sigma_{\mathrm{dn}}^4. \tag{23}$$

The phase uncertainty is now given by

$$\Delta\theta_{\mathrm{gdn}} = \frac{\sqrt{\langle \hat{J}_z^4 \rangle_{\mathrm{gdn}} - \langle \hat{J}_z^2 \rangle_{\mathrm{gdn}}^2}}{\sqrt{\nu}\left|\frac{\mathrm{d}\langle \hat{J}_z^2 \rangle}{\mathrm{d}\theta}\right|}, \tag{24}$$

where $\mathrm{d}\langle \hat{J}_z^2 \rangle_{\mathrm{gdn}} / \mathrm{d}\theta = \mathrm{d}\langle \hat{J}_z^2 \rangle / \mathrm{d}\theta$.

In figure 4 we show the phase uncertainty $\Delta\theta_{\mathrm{gdn}}$ with respect to shot-noise in a molecular interferometry, for different values of the detection noise σ_{dn} and the interaction parameter $1/(k_F a)$. As a general trend, the phase uncertainty increases with the detection noise. Particularly, the Heisenberg limit can not be achieved for $\sigma_{\mathrm{dn}} > 0$, and the precision do not beat the standard quantum limit for very small values of θ. The maximum precision (minimum phase uncertainty) is obtained approximately when $\langle \hat{J}_z^2 \rangle \sim \sigma_{\mathrm{dn}}^2$, as for interferometers of atomic BECs [6]. The impact of the partially fermionic behavior for small detection noise is also small, while for larger values of the detection noise, the deviation from ideal bosonic interferences can not be neglected. For instance, for $\sigma_{\mathrm{dn}} = 1$ the relative difference in gain between the atomic and the molecular interferometry at $1/(k_F a) = 1$ and $\theta = 0.055$ (minimum phase uncertainty) is $|G_{\mathrm{mol.}} - G_{\mathrm{at.}}|/G_{\mathrm{at.}} \approx 0.065$, while for $\sigma_{\mathrm{dn}} = 2.5$ the relative gain difference is 0.31 at $\theta = 0.165$. These values are indicated with gray arrows in figure 4.

6. Conclusion

In this work we have shown the impact of the underlying fermionic structure of ultracold molecules in the interference of two mBECs for entanglement enhanced precision measurement. We assume initially prepared entangled twin Fock state of mBECs at zero temperature, for which the Heisenberg limit can be achieved, and an interferometric dynamics characterized by a single global parameter θ. To compute the initial state we use an ansatz of composite bosons which carries with all possible particle exchanges (for the identical fermions) and all interactions between different fermion species. This allowed us to faithfully describe the effects of fermion exchanges on the phase uncertainty estimation in high precision experiments using mBECs.

The deviation from the ideal bosonic behavior in the interference of composite particles is a consequence of the condensate quantum depletion, and can be interpreted as a partially fermionic behavior [32]. This partially fermionic contribution, due to Pauli blockade between identical fermions, reduce the even/odd particle fluctuations, while the U-shape of the distribution of population imbalance is preserved. As a consequence, the precision gain decreases and the Heisenberg limit is not achieved for non-negligible values of the depletion ($1/(k_F a) \approx 1$). Moreover, the detection noise enhances the impact of the partially fermionic contribution which significantly affect the precision gain for inefficient detectors. Nevertheless, molecular interferometers with highly efficient detectors would allow high metrological precision comparable to atomic interferometers. Finite temperature ($T \neq 0$) effects should also be considered for real experiments. The finite temperature usually increases depletion in both fermionic [18] and bosonic [39] gases and it also would affect the formation of pairs making the coboson ansatz less efficient. If the temperature is sufficiently low, quantitatively lower than the Fermi temperature, our results remain correct, but in general the effect of the temperature would result in a loss of the metrological precision [40].

Progress on atomic and molecular BEC physics are gapped by at least 10 years. Since particles of the former are bosonic atoms and the later fermionic atoms the physics by which Bose–Einstein condensation emerge is quite different. In fact these differences could be advantageous once the BEC stage is attained, since molecular BECs have a lifetime of approximately 20 s, much longer than the lifetime of atomic BEC existing for just one second [41]. On the other hand, the internal state of bosonic atoms can be tunned relatively easy, which allowed the preparation of high entangled twin Fock state of BECs [6, 7]. The more natural way to produce entangled states in particle number for molecular interferometers is reducing particle fluctuations in a double well potential, as carried out with ultracold bosonic atoms almost 10 years ago [42]. Finally, given the general character of our theory, the proposed interferometric process for entanglement enhanced metrology can be extended to interacting fermions in optical lattices [32, 43–45]. In fact, our proposed interference dynamics could be implemented experimentally by tunning differently the tunneling rate between sites along the x and y directions of a two-dimensional optical lattice [32, 44].

Acknowledgments

We thank Malte Tichy and Klaus Mølmer for stimulating discussions. We thank the CSIRC of the University of Granada for providing the computing time in the Alhambra supercomputer. IR is grateful for the hospitality of the Quantum Information Group at ETHZ, where this work has been completed. PAB, FF and IR gratefully acknowledges support by the Conselho Nacional de Desenvolvimento Científico e Tecnológico do Brasil. PAB and APM acknowledge funding from grant PICT-BID 2017-2583 from Agencia Nacional de Promoción Científica y Tecnológica de Argentina. APM acknowledges grant GRFT-2018 MINCYT-Córdoba. This study was partially financed by the Coordenação de Aperfeiçoamento de Pessoal de Nível Superior—Brasil (CAPES)—Finance Code 001.

ORCID iDs

P Alexander Bouvrie https://orcid.org/0000-0002-9280-6540
Ana P Majtey https://orcid.org/0000-0001-5447-8032
Itzhak Roditi https://orcid.org/0000-0003-2363-5626

References

[1] Schnabel R, Mavalvala N, McClelland D E and Lam P K 2010 *Nat. Commun.* **1** 121
[2] Aasi J *et al* 2013 *Nat. Photon.* **7** 613
[3] Xiao M, Wu L A and Kimble H J 1987 *Phys. Rev. Lett.* **59** 278–81
[4] Holland M J and Burnett K 1993 *Phys. Rev. Lett.* **71** 1355–8
[5] Spasibko K Y, Töppel F, Iskhakov T S, Stobińska M, Chekhova M V and Leuchs G 2014 *New J. Phys.* **16** 013025
[6] Lücke B *et al* 2011 *Science* **334** 773–6
[7] Luo X Y, Zou Y Q, Wu L N, Liu Q, Han M F, Tey M K and You L 2017 *Science* **355** 620–3
[8] Zou Y Q, Wu L N, Liu Q, Luo X Y, Guo S F, Cao J H, Tey M K and You L 2018 *Proc. Natl Acad. Sci.* **115** 6381–5
[9] Greiner M, Regal C A and Jin D S 2003 *Nature* **426** 537
[10] Jochim S, Bartenstein M, Altmeyer A, Hendl G, Riedl S, Chin C, Hecker Denschlag J and Grimm R 2003 *Science* **302** 2101–3
[11] Whitfield J 2003 Nature news, Molecules form new state of matter https://nature.com/news/2003/031110/full/news031110-16.html
[12] Jochim S 2004 Bose–Einstein Condensation of Molecules *PhD Thesis* University of Innsbruck
[13] Chin C, Grimm R, Julienne P and Tiesinga E 2010 *Rev. Mod. Phys.* **82** 1225–86
[14] Giorgini S, Pitaevskii L P and Stringari S 2008 *Rev. Mod. Phys.* **80** 1215–74
[15] Zwierlein M W, Stan C A, Schunck C H, Raupach S M F, Kerman A J and Ketterle W 2004 *Phys. Rev. Lett.* **92** 120403
[16] Astrakharchik G E, Boronat J, Casulleras J and Giorgini S 2005 *Phys. Rev. Lett.* **95** 230405
[17] Bouvrie P A, Tichy M C and Roditi I 2017 *Phys. Rev.* A **95** 023617
[18] Kohstall C, Riedl S, Sánchez Guajardo E R, Sidorenkov L A, Denschlag J H and Grimm R 2011 *New J. Phys.* **13** 065027
[19] Combescot M, Betbeder-Matibet O and Dubin F 2008 *Phys. Rep.* **463** 215–320
[20] Bourdel T, Khaykovich L, Cubizolles J, Zhang J, Chevy F, Teichmann M, Tarruell L, Kokkelmans S J J M F and Salomon C 2004 *Phys. Rev. Lett.* **93** 050401
[21] Combescot M, Shiau S Y and Chang Y C 2016 *Phys. Rev.* A **93** 013624
[22] Shiau S Y, Combescot M and Chang Y C 2016 *Phys. Rev.* A **94** 052706
[23] Combescot M, Leyronas X and Tanguy C 2003 *Eur. Phys J.* B **31** 17–24

[24] Law C K 2005 *Phys. Rev.* A **71** 034306
[25] Tichy M C, Bouvrie P A and Mølmer K 2014 *App. Phys.* B **117** 785
[26] Serwane F, Zürn G, Lompe T, Ottenstein T B, Wenz A N and Jochim S 2011 *Science* **332** 336–8
[27] Zürn G, Wenz A N, Murmann S, Bergschneider A, Lompe T and Jochim S 2013 *Phys. Rev. Lett.* **111** 175302
[28] Murmann S, Bergschneider A, Klinkhamer V M, Zürn G, Lompe T and Jochim S 2015 *Phys. Rev. Lett.* **114** 080402
[29] Tichy M C, Bouvrie P A and Mølmer K 2012 *Phys. Rev.* A **86** 042317
[30] Bouvrie P A, Tichy M C and Mølmer K 2016 *Phys. Rev.* A **94** 053624
[31] Bouvrie P A, Cuestas E, Roditi I and Majtey A P 2019 *Phys. Rev.* A **99** 063601
[32] Tichy M C, Bouvrie P A and Mølmer K 2012 *Phys. Rev. Lett.* **109** 260403
[33] Tichy M C, Lim H T, Ra Y S, Mintert F, Kim Y H and Buchleitner A 2011 *Phys. Rev.* A **83** 062111
[34] Tichy M C, Tiersch M, Mintert F and Buchleitner A 2012 *New J. Phys.* **14** 093015
[35] Laloë F and Mullin W 2012 *Found. Phys.* **42** 53–67
[36] Benatti F, Floreanini R and Marzolino U 2014 *Phys. Rev.* A **89** 032326
[37] Kim T, Pfister O, Holland M J, Noh J and Hall J L 1998 *Phys. Rev.* A **57** 4004–13
[38] Gross C 2012 *J. Phys. B: At. Mol. and Opt. Phys.* **45** 103001
[39] Lopes R, Eigen C, Navon N, Clément D, Smith R P and Hadzibabic Z 2017 *Phys. Rev. Lett.* **119** 190404
[40] Esteve J, Gross C, Weller A, Giovanazzi S and Oberthaler M K 2008 *Nature* **455** 1216–9
[41] Becker D *et al* 2018 *Nature* **562** 391–5
[42] Gross C, Zibold T, Nicklas E, Estève J and Oberthaler M K 2010 *Nature* **464** 1165–9
[43] Shiau S Y, Chenu A and Combescot M 2019 *New J. Phys.* **21** 043041
[44] Céspedes P, Rufeil-Fiori E, Bouvrie P A, Majtey A P and Cormick C 2019 *Phys. Rev.* A **100** 012309
[45] Lasmar Z, Bouvrie P A, Sajna A S, Tichy M C and Kurzynski P 2019 *Phys. Rev.* A **100** 032105